Tr. J. of Physics
22 (1998) , 955 – 970.


# Optical Anisotropy of Iron Garnets With Growing Anisotropy

**Odil OCHILOV**
*Optics Laboratory Research Institute of Applied Physics*
*Tashkent State University Tashkent - UZBEKISTAN*

Received 08.12.1995

**Abstract**

The theoretical analysis of the position of principal diachronic directions at magnetization rotation in (100) and (110) planes for the case of growing dichroism axes in random directions was made. The calculations of angular dependencies of dichroic axes (DA) position for different values of the magneto-optical anisotropy parameter, $a$, have been done. The relations between the growing and magneto-optical dichroism, $K/M$, and the angle $\delta$ characterizing the direction of principal growing dichroism axes were given. The angular dependences of $DA$ position in epitaxial iron garnet films have been investigated experimentally. The measurements at the different light wavelengths permitted one to vary extensively the $a$ and $K/M$ parameters and to show that the experimental dependences are described successfully by the expressions obtained.

## 1. Introduction

Iron garnets crystallize in a cubic structure and, consequently, to first approximation, are to be optically isotropic. However, investigations conducted during the last twenty five years have shown that some optical phenomena observed in the crystals, such as linear dichroism, have shown optical anisotropy. In this connection the different mechanisms of observed anisotropy are possible:

1. Anisotropy source can be the quadratic magneto-optical effect of magnetic linear birefringence or dichroism, which induces the optical indicatrix deformation to depended on the magnetization orientation in the crystal. The phenomenon had been studied intensively theoretically and experimentally and typical results have been given in review works [1-6].

2. Soon after the synthesis of the iron garnets contained the cylindrical magnetic domains it has been elucidated that such materials side by side with growing magnetic

anisotropy have growing optical anisotropy (GOA), which can be observed in both birefringence and dichroism [10-14]. Subsequently, it has been found that the GOA appears both in epitaxial iron garnet films and the bulk crystal. And the GOA has been observed in birefringence [15, 16] and dichroism [17].

3. Optical anisotropy can appear due to the fourth order terms on magnetization. Contribution of such terms into the iron garnets birefringence has been found experimentally in works [8, 9], where they found that the fourth order terms on magnetization were involved to explain the untypical linear dichroism at the absorption band region for the rare-earth ion in europium iron garnet.

4. The source of optical anisotropy in cubic crystals can be the terms which take account of the spatial dispersion in itself (which, apparently, was not observed experimentally in (ferro-magnetics) or simultaneous spatial dispersion and magnetization. The last mechanism has been used by [9] to explain the absorption anisotropy of europium iron garnets with the direction of light propagation along and perpendicular to magnetization.

In the present work, we examine the optical anisotropy of iron garnets caused by linear dichroism. In general, the dichroism is connected with both the random magnetization and the growing crystal and film anisotropy. In section 2 we dwell on relations characterizing the turn of the dichroic axes with rotation of the magnetization in crystals with the GOA. In section 3 the experimental results of magneto-optical anisotropy spectroscopic investigations in some epitaxial iron garnets films and the results on ichroic axes in the films are given. In section 4, an analysis of the obtained results and also of data from available literature are represented.

## 2. Dichroic Axes Rotation in Cubic Magnetics with Growing Optical Anisotropy

Rotation of principal optical indicatrix directions in cubic magnetics with magnetization rotation in the principal symmetry planes has been examined in works [3, 4]. And the rotation has been studied in transparenty region in yttrium iron garnet and ytterbium iron garnet [18] and erbium iron garnet [20]. In the absorption region dichroic axes rotation occurs at the same time with optical indicatrix rotation, which are defined as the directions in the crystal where the absorptions are either maximum or minimum with the light polarization parallel to them. Theoretical and experimental investigations of dichroic axes rotation in impure absorption and intrinsic absorption regions in iron garnets have been conducted in works [21, 24] and [25] respectively.

In all this work on the rotation of principal directions of optical indicatrix and dichroic axes it has been supposed that the optical anisotropy is caused only by random magnetization. However, in many cases, in crystals and films the GOA occurs, as we will show in this chapter, and can essentially influence the principal directions and dichroic axes rotation with magnetization rotation. We will analyze two principal crystallographic (100) and (110) planes for the cubic crystal. At the beginning we will consider the optical indicatrix motion at magnetization rotation and then we will derive the general expressions for the GOA case with arbitrary direction of its principal axes. The change of optical in-

dicatrix coefficients in the cubic ferromagnetic with magnetization can be given as follows [7]:

$$\begin{bmatrix} B_1 - B_0 \\ B_2 - B_0 \\ B_3 - B_0 \\ B_4 \\ B_5 \\ B_6 \end{bmatrix} = \begin{bmatrix} \Delta B_1 \\ \Delta B_2 \\ \Delta B_3 \\ \Delta B_4 \\ \Delta B_5 \\ \Delta B_6 \end{bmatrix} = \begin{bmatrix} \rho_{11}\alpha_1^2 + \rho_{12}\alpha_2^2 + \rho_{13}\alpha_3^2 \\ \rho_{12}\alpha_1^2 + \rho_{11}\alpha_2^2 + \rho_{12}\alpha_3^2 \\ \rho_{12}\alpha_1^2 + \rho_{12}\alpha_2^2 + \rho_{11}\alpha_3^2 \\ \rho_{44}\alpha_2\alpha_3 \\ \rho_{44}\alpha_3\alpha_1 \\ \rho_{44}\alpha_2\alpha_1 \end{bmatrix}, \tag{1}$$

where $B_i = \partial E_i/\partial D_i$ are the dielectric inpermeabilities, $\rho_{ijk\ell}$ is the magnetooptical four-rank tensor symmetric on the pair of indexes, and $\alpha_{\kappa\ell}$ are the direction cosines of magnetization. The presence of the terms $B_4, B_5, B_6$ in the indicatrix equation testifies that the reference system of axes is not more the principal, that is they do not coincide with the crystallographic four order axes with the optical ellipsoid axis. Using a typical method such equation might be reduced to the canonical form by rotaring the system of axes, in arbitrarily the receipt of any information from the transformation formulae is not possible. It is important to consider lens indicatrix rotation with magnetization motion in the symmetry planes.

1. $\vec{m} \perp [110], \vec{k}|[110], \alpha_1 = \alpha_2 \neq 0, \alpha_3 \neq 0$

All three direction cosines are differed from zero and all six coefficients are changed at magnetization motion in (110) planes [7]. These changes are described as

$$\begin{aligned} \Delta B_1 &= \vec{m}^2[(\rho_{11} + \rho_{12})\alpha_1^2 + \rho_{12}\alpha_3^2]; \qquad & \Delta B_4 &= \vec{m}^2\rho_{44}\alpha_2\alpha_3; \\ \Delta B_2 &= \vec{m}^2[(\rho_{11} + \rho_{12})\alpha_1^2 + \rho_{12}\alpha_3^2]; \qquad & \Delta B_5 &= \vec{m}^2\rho_{44}\alpha_1\alpha_3; \\ \Delta B_3 &= \vec{m}^2[(2\rho_{12})\alpha_1^2 + \rho_{11}\alpha_3^2]; \qquad & \Delta B_6 &= \vec{m}^2\rho_{44}\alpha_1^2. \end{aligned} \tag{2}$$

All of the indicatrix components are differed from zero; and to lead to the principal axes we will turn the axes by 45° around the [001] axis from the [100] and [010] directions.

$$\{B'\} = \begin{pmatrix} B_1 + B_6 & 0 & \sqrt{2}B_4 \\ 0 & B_2 - B_6 & 0 \\ \sqrt{2}B_4 & 0 & B_3 \end{pmatrix}. \tag{3}$$

Now, the indicatrix, $\{B\}$, might lead to the diagonal form by a rotation about the [100] axis through an angle of $\theta$ defined by the relation

$$tg2\theta = \frac{2\sqrt{2}B_4}{B_3 - B_1 - B_6}. \tag{4}$$

2. $\vec{m} \perp [100], \vec{k}|[100], \alpha_1 \neq 0, \alpha_2 = 0, \alpha_3 \neq 0.$

In this case, using (1) we find

$$\begin{aligned} \Delta B_1 &= \vec{m}^2(\rho_{11} + \alpha_1^2 + \rho_{12}\alpha_3^2); \qquad & \Delta B_4 &= 0; \\ \Delta B_2 &= \vec{m}^2(\rho_{11}\alpha_1^2 + \rho_{12}\alpha_3^2); \qquad & \Delta B_5 &= \vec{m}^2\rho_{44}\alpha_1\alpha_3; \\ \Delta B_3 &= \vec{m}^2(\rho_{11}\alpha_1^2 + \rho_{11}\alpha_3^2); \qquad & \Delta B_6 &= 0. \end{aligned} \tag{5}$$

The optical indicatrix leads to the principal axes via a rotation, $\theta$, the axes systems around the [100] axis which has a tangent determined by the equation:

$$tg2\theta = \frac{2B_5}{B_1 - B_3}. \tag{6}$$

Formulae (5, 6) describe only the magnetic contribution. Now we consider the contribution of the growing dichroism. Let us assume that the principal directions of growing dichroism do not coincide with the symmetry axes and are under some angle, $\delta$, with respect to the [100] axis in (110) plate (Fig. 1). In system of axes 1, 2 coupled with the principal directions of growing dichroism the expression for indicatrix of the growing contribution is expressed as:

$$T_{ij} = \begin{bmatrix} K & 0 \\ 0 & K \end{bmatrix}. \tag{7}$$

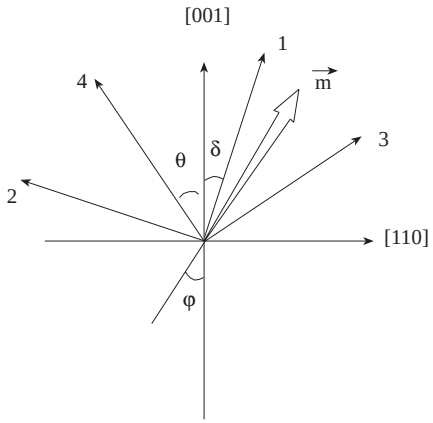


**Figure 1.** System of axes, reading of angles and dichroic axes rotation at magnetization motion in (110) plate: 1,2 - crystallographic dichroic axes; 3,4 - total effects axes

To be more convenient we take the system of axes coupled with crystallographic directions. In these axes the equation is defined as:

$$T_{ij} = a_{ik}a_{j\ell}T_{k\ell}, \tag{8}$$

where $T_{k\ell}$ is the rotation matrix with respect to the crystallographic axes. Taking into account the growing contribution the indicatrix equation can be written by follows:

$$\{B'\} + T'_{ij} = \{B''\}. \tag{9}$$

Now the indicatrix $\{B''\}$ can be led to the diagonal form by rotation around the [100] or [110] axes on the angle of $\theta$, which has a tangent determined by the diagonal and off-diagonal indicatrix components noted as follows:

1. $\vec{m} \perp [100], \vec{k}|[100]$

$$tg2\theta = \frac{\sin 2\varphi + (2K/M)\sin 2\delta}{1/a^*(\cos 2\varphi) + (2K/M)\cos 2\delta} \tag{10}$$

where $\varphi$ is the angle between the magnetization $\vec{m}$ and the [001] axis; $a = \rho_{44}/(\rho_{11} - \rho_{12})$ is the magnetooptic anisotropy coefficient; $M = \rho_{44}\vec{m}_2$ is the magnetic contribution value, $K = (\alpha_1 - \alpha_2)$ is the growing dichroism value and $\alpha_1 = \cos\varphi$.

With the absence of growing dichroism, $K = 0$ and expression (10) is modified into the formula:

$$tg2\theta = atg2\varphi, \tag{11}$$

as obtained earlier in [19] for the cubic crystals. In another extreme case where $M = 0$, the dichroic axes position coincides with the growing dichroism axes and does not depend on the magnetization orientation. In intermediate cases the dichroic axes position depends on the concrete relations between parameters $K, M$ and $a$. Fig. 2 shows, as illustration, the results of calculations on axes rotation for some specific relations between these parameters.

2. $m \perp [110], k|[110]$

The expression for angle $\theta$ for the magnetization motion in (110) plane is assumed to be followed by:

$$tg2\theta = \frac{\sin 2\varphi + (2K/M)\sin 2\delta}{1/a(\cos 2\varphi) + (1-a)/2a(\sin^2\varphi) + (2K/M)\cos 2\delta}. \tag{12}$$

The results of calculations in accordance with the formula for some specific relations between the parameters $K, M$ and $a$ are given in Fig. 3. The calculations show that as $K/M$ rises with the growing dichroism, the $\theta(\varphi)$ dependences varied qualitatively. At $K/M = 0$, these dependences have 90-periodicity, at $K/M < 1$ the periodicity is close to 90-periodicity, but at further rising of the relation $K/M > 1$ the periodicity gradually transforms into 180-periodicity and the amplitude of change, $\theta(\varphi)$, decreases. The form of the dependences is determined by the value of parameter $a$ and angle $\delta$, which define the initial dichroic axes position at $\varphi = 0$.

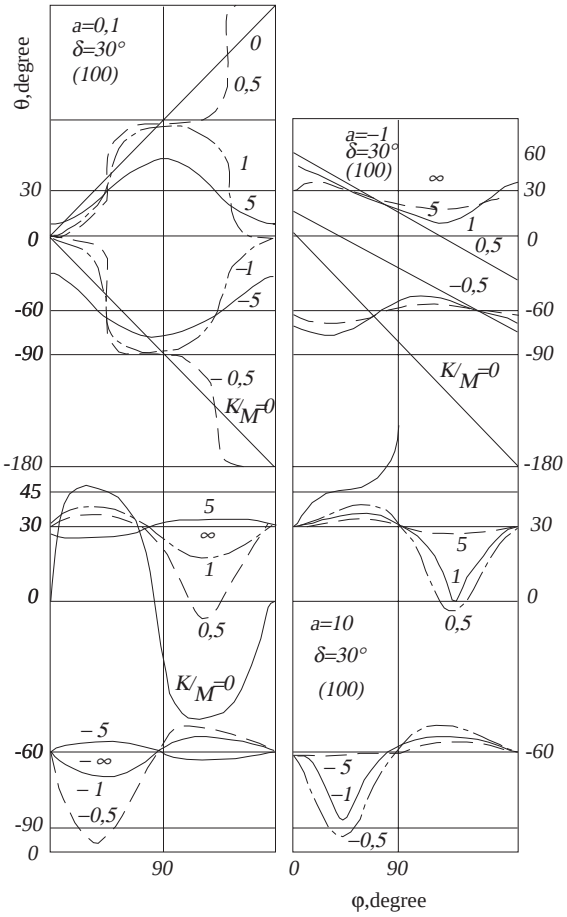


**Figure 2.** Dichroic axes motion at magnetization rotation in (100) plane at the different relations $K/M, a$ and $\delta$.

## 3. Experimental Results

Magnetic linear dichroism (MLD) spectra and dichroic axes rotation have been investigated on the samples of epitaxial iron garnet films of different compounds $Y_3Fe_5O_{12}$, $(YBi)_3(FeGa)_5O_{12}$ and $(YPr)_3(FeGa)_5O_{12}$.

The films have been grown on the gadolinium gallium garnet $Gd_3Ga_5O_{12}$ substrates cut out of the symmetry (100) and (110) planes. The arrangement used to measure the dichroism and dichroic axes rotation has been described in [17, 25]. The important feature of the arrangement has been as follows: magnetic field by value of $3kOe$ could be applied to a sample in any direction and the sample could be turned around direction of

light propagation. The features of arrangement permitted one to separate the magnetic and elastic linear dichroisms from each other and also to determine the dichroic directions position with precision of about 2°.

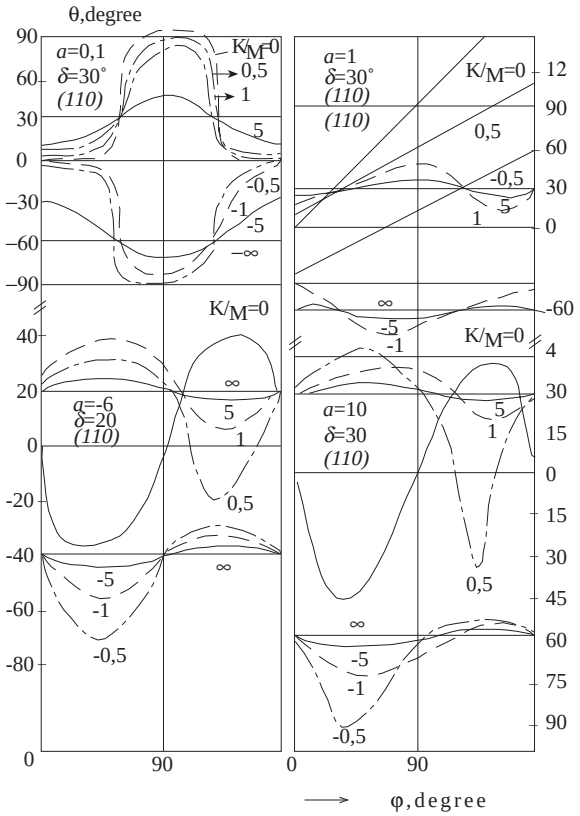


**Figure 3.** Dichroic axes motion at magnetization rotation in (110) plane at the different relations $K/M, a$ and $\delta$

Growing optical dichroism (GOD) spectral dependences in YIG and *Bi*-substituted YIG at room temperature are represented in Fig. 4. As one can see from the figure a number of maximums at $19500cm^{-1}, 20500cm^{-1}, 21100cm^{-1}$ and $21700cm^{-1}$ is observed in the GOD YIG spectrum. The corresponding MLD maximums on these frequencies are also observed in pure YIG. It testifies that the transitions in iron ions are displayed in the GOD film of substituted garnets. In contrast to YIG in *Bi*-substituted garnet the GOD spectrum is not as well resolved and the monotonous GOD increase is observed. The features of corresponding transitions in iron ions are shown in the spectra as the feebly marked bends.

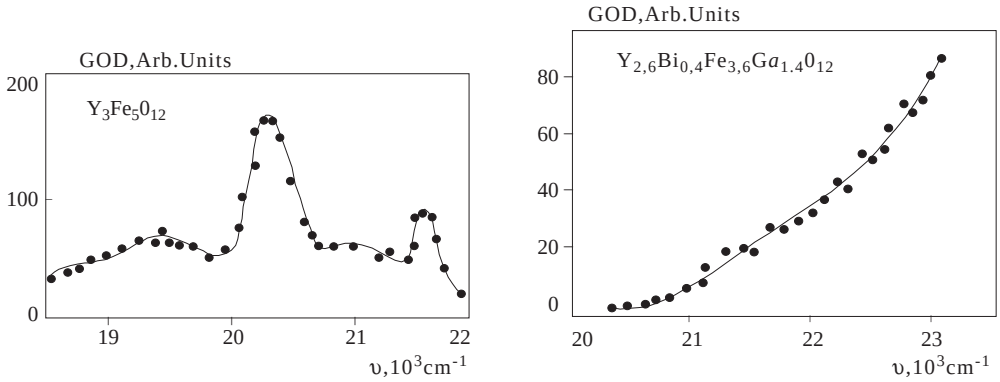


**Figure 4.** The GOD spectral dependence in the epitaxial films. $\vec{k}||110$, $T = 295K$.

MLD spectra of the examined films for two principal magnetization orientations are given in Fig. 5, where the yttrium iron garnet MLD spectra are also given to be compared.

Fig. 5 shows, that the magnetooptical anisotropy parameter, $a$, strongly depends on the wavelength, that is shown in the dichroic axes rotation.

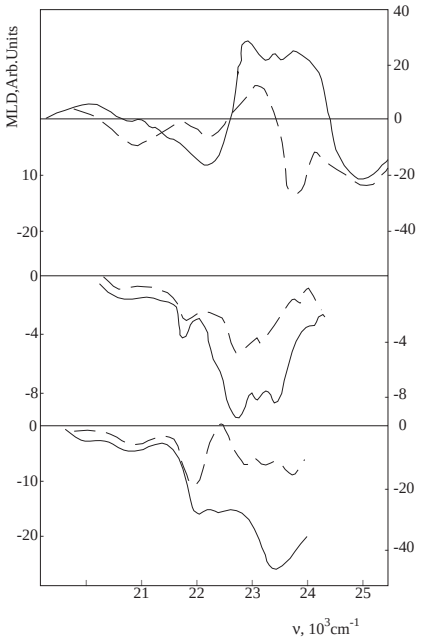


**Figure 5.** The MLD spectral dependence in iron garnets films: solid curve $-\lambda_2 m^2$, dashed curve -$(\lambda_2 + \lambda_3)m^2$ a) for $Y_3Fe_5O_{12}$, b) $(YBi)_3(FeGa)_5O_{12}$ c) $(YPr)_3(FeGa)_5O_{12}$

The dichroic axes rotation is shown in Fig. 6a at the different light frequencies, that is for different values of parameter $a$ in the (100) film of iron garnet compound $(YPr)_3(FeGe)_5O_{12}$. Growing dichroism in the film was absent and in accordance with the relation (11) the dependences $\theta(\varphi)$ had 90-periodicity. The calculated curves describe the observed experimental dependences in good agreement.

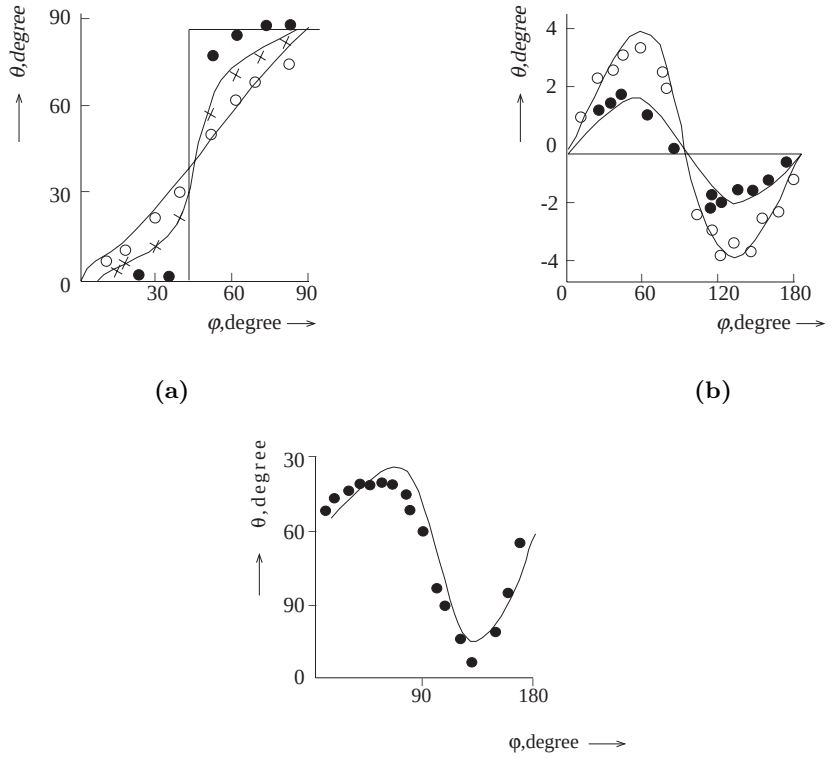


**Figure 6.** Dependences of dichroic axes rotation on magnetization position: a) in (100) plane in $(YP_2)_3(FeGa)_5O_{12}, a = 0$ (dots) and $v = 19690cm^{-1}, a = 0,1$ (crossed) and $v = 20600cm^{-1}, a = 0,2$ (light circles) and $v = 21700cm^{-1}$; b) in (110) plane in $(YBi)_3(FeGa)_5O_{12}, a = 1, K/M = 7$ (light circles) and $v = 20700cm^{-1}, a = 2, K/M = 1,5$ (dots) and $v = 21900cm^{-1}$; c) in (110) plane in $Y_3Fe_5O_{12}, a = 5,5, 2K/M = 0,87$ (dots) and $v = 20690cm^{-1}$. Solid curves are calculated according to the formulae for the (110) plane (4) and the (100) plane (5)

The dependences $\theta(\varphi)$ for the (100) film of $(YBi)_3(FeGa)_5O_{12}$ iron garnet are given in Fig. 6b. Great growing elastic dichroism occurred in the film. The principal dichroism directions have been coincided with the crystallographic [110] axes. This circumstance has caused the 180-periodicity of the dependence $\theta(\varphi)$. In the film the experimental

results are successfully described by curves obtained according to formula (10) at the corresponding values of parameter $a$ and relation $K/M$.

In the film of compound $Y_3Fe_5O_{12}$ grown in the (110) plane the principal growing dichroism directions did not coincide with crystallographic axes. Dichroism axes motion in this film is shown in Fig. 6c. Here, the dependence $\theta(\varphi)$ has the 180-periodicity and oscillates around the position corresponding to one of the principal growing dichroism directions. This dependence is described successfully by formula (11) for the (110) plane. It should be noted, that parameters $a, M, K$ and $\delta$ involved in relations (10) and (11) can be found from independent experiments and can be used to calculate the dichroism axes motion.

## 4. Discussion on Results

The GOD in the substituted rare-earth iron garnet films can obviously appear for two reasons:

1. Inaccurable coupling of the substrate and the film, since the last one might be in the stressed state. In literature on the experimental data base the model of homogeneously deformed (stretched or compressed) on the film thickness and strongly distorted transition small thickness layer has been proposed [16]. If we neglect the influence of the thin transition layer on the optical properties [26, 27] the GOD would not appear in this model in the (111) or (100) plates. The appearance of this dichroism in the experiment can be related to both the transition layer influence and inaccurate substrate plane orientation. In principle, the separation of the two mechanisms is possible by studying the GOD value dependence on the film thickness for a gradual decrease of this thickness. In the present case, if the reason for the destroyed is the destructed thin layer, the thickness decrease did not influence on the effect quantity, otherwise the effect depended on the film thickness linearly.

2. The GOD source can be, in principle, a mechanism as proposed by Sturge and Van der Ziel [13], according to which a REIG displaced compound rising in a specific plane the rare-earth ions exhibit a tendency to occupy the specific dodecahedron positions. As result, the rare-earth ions are inhomogeneously distributed on dodecahedrons and it denatures the crystal symmetry below the cubic one. However, such mechanism leads, first, to the optical dichroism on the transitions in the rare-earth ions, and at minimum, to influence the transitions of iron ions which, nevertheless, have substrates with cubic symmetry. Observation of the maximums corresponding to the frequency in the OD and MLD spectra in YIG gives evidence that the iron ion transitions exist in the GOD films of substituted above. In contrast to the YIG, in the $Bi$-substituted garnet, as we have mentioned, the OD spectrum is resolved worse and the OD monotonic rise is observed. The features of corresponding transitions in iron ions are displayed in the as feebly marked bends. The picture can concerned with the long "tail" position in the spectrum from the more high energy states. Substitution by $Bi$ in the garnet lattice influences essentially on the garnet electronic structure, as the data on absorption and the MCD (magnetic crystallographic dichroism) spectra have shown [29-31]. Evidently,

it is displayed in the OD spectral dependence of the $Bi$-substituted films. Now, this results can be considered as a qualitative, but, obviously, such method can be used to study and to interpretate the electronic levels in the films for specific deformation values. Moreover, a separation by contribution in the OD films of the destructed layer effect and the homogeneous deformation is seemed to be of interest.

b) Substitution of $Y$ ions in $Y_3Fe_5O_{12}$ by $Bi$ and $Pr$ ions leads to an increase of Faraday Rotation (FR) in the infrared spectral region (where the transparency window is observed). It then suggests that the materials may be used in a different type of magne tooptical apparatus. Besides the FR increase, in the $Bi$- and $Pr$-substituted garnets, the rotation sign is observed to change in comparison with $Y_3Fe_5O_{12}$. In work [28] we have shown that FR sign change in the transparency region is involved with the negative MCD $(16000 - 26000cm^{-1})$ region and, primarily, to the strong rising of the $22000cm^{-1}$ line in the region.

Investigations of the MLD quadratic effect on magnetization in $Bi$- and $Pr$-substituted iron garnets in the above mentioned spectral region have shown that, as for other magnetooptical effects, the $Bi$ and $Pr$ substitution in the $Y_3Fe_5O_{12}$ leads to the strong MLD spectrum changes in comparison with the MLD spectrum in $Y_3Fe_5O_{12}$. Indeed, comparing the MLD spectra in the pure YIG and $Bi$- and $Pr$-substituted YIG we can find the following main features (see Fig. 5):

1. In all of the garnets the MLD spectrum is observed both substitutions (except some particular cases, for example, $22400cm^{-1}$ in the $Pr$-substituted garnet).

2. In the range of $20000 - 24000cm^{-1}$ the $Bi$- and $Pr$-substituted garnets MLD spectrum is characterized by the octahedral component predomonation that, in principle, can give evidence of the primary reinforcement of magnetooptical activity and octahedral transitions.

3. In contrast to YIG, which has few sign changes in the region, on a frequency, the MLD sign in the $Bi$- and $Pr$-substituted garnet is not changed in the investigated region.

4. In the MLD spectra of all garnets the features are observed approximately at the same frequencies. So, we can establish, that $Bi$- and $Pr$-ions substitution in the garnet lattice changes strongly the MLD anisotropy in the same spectral region, where $Fe$ ion transitions in the octahedral and tetrahedral surroundings are observed. It is logical to propose the ion influence is displayed primarily by the $Fe$ ions, which are closer to them. It should be taken into account, that the influence is rather strong and, particularly, the strong variation of the MCD spectra, FR and etc. caused by even small $Bi$- and $Pr$- ions additions in the YIG exposes the phenomenon [35, 36].

To explain the anomalous activity in $Bi$- and $Pr$-substituted garnets a number of mechanisms have been proposed [32, 35]. An increase of spin-orbital splitting of the excited state (due to the great spin-orbital constant of $Bi$) and an increase of exchange interaction between the iron sublattices are the most probable explorations. The temperature, $T_k$, rising in $Bi$-substituted iron garnets gives evidence of the latter interaction [35, 36].

However, the concrete exchange interaction reinforcement mechanism between the iron sublattices at substitution of the $Y$ ions by the $Bi$ ions is still unclear.

In the $Pr$-substituted garnets the exchange interaction increase between the sublattices might be effective because of substitution of the $Y$ ions by the $Pr$ ions that have a greater size. It can lead to the angle increase between the iron sublattices.

The influence of $Pr^{3+}$-ions on magnetooptical transitions activity in $Fe^{3+}$ ions might occur, first by means of exchange reinforcement between the iron sublattices (having substitution of $Y^{3+}$-ions, which have a greater side the angel in $[Fe^{3+}_{okt}] - O^{-2} - [Fe^{3+}_{tet}]$ might be increased), second, by means of the splitting increase $\Delta\omega$, evidently, as in the $Bi$ substituted iron garnets is affected by the mixing of $Pr^{3+}$-ions wavefunctions and iron wave functions [37].

So, in the $Bi^{3+}$- and $Pr^{3+}$-substituted IG the abnormal FR is induced by the reinforcement and optical transitions character change in $Fe^{3+}$ ions.

The changes are displayed not only in MCD spectra [33], but strong MLD spectral changes also occur. To make clear the concrete microscopic mechanism of $Bi$ and $Pr$ influence on optical transitions in the garnets a detailed theoretical investigation be very desirable.

So, our investigations and calculations testify to the necessity of taking into account the growing optical anisotropy, where it occurs with magnetooptical second order effect analysis, such as the magnetic linear dichroism and the magnetic linear birefringence (MLB). The growing optical anisotropy can influence the angular dependences and the observed effect magnitude. The growing elastooptical anisotropy can be present not only in the epitaxial films, but in the iron garnet monocrystal, as it has been observed in works [7, 38]. In our opinion, a sufficient criterion for the absence of growing elastooptical anisotropy in cubic crystal occurs under the following condition for the magnetic linear dichroism, $\Delta\alpha$, measured, for example, in the monocrystal plate or the epitaxial (110) film:

$$\Delta\alpha_{110} = 1/2(\Delta\alpha_{100}) + \Delta\alpha_{111}), \tag{13}$$

where the lower index points out the magnetization direction in the sample plane. The analogous relationship is correct for magnetic linear birefringence $\Delta n_{110}$. These conditions are the direct consequence of a phenomenologica analysis of second order magnetooptical effects in cubic crystals [39]. Nonfulfilment of these conditions gives evidence of the growing optical anisotropy and it should be taken into account when analizing experimental results.

Obviously, the growing optical anisotropy has occured in erbium iron garnet crystals, in which magnetic linear birefringence has been studied [20]. From Fig. 1 and 2 in the work it follows that $\Delta n_{110} > \Delta n_{100} > \Delta n_{111}$ for the (110) plate. But it contradicts the above mentioned criterion for the cubic crystals. In the work the mistaken conclusion on non-usage of simple phenomenologica analysis to multisublattice magnetics with motion analysis of principal indicatrix and optical axe directions has been made. In our opinion, the mistake of the authors consists in confusion of ideas as the principal indicatrix direction and the optical indicatrix axis. As it follows from their investigation method description [20], the principal directions positions has been studied and with the analysis the conclusions of the work [21] for optical axes have been used. In connection with this, the

conclusions on the difference of results with the calculations based on phenomenologica theory [20] are considered by us as possibly incorrect.

It is important to note, that at the analysis of the dichroic axes orientation dependences in the cubic crystals it is necessity to take into account the probable CLD (crystallographic linear dichroism) contribution arising due to the crystal imperfection (internal stress, dislocation and etc.). In particular, evidently, these circumstances explain the different character of such dependences obtained in the works [21, 22] for *Sn*- and *Sb*-doped YIG in the impure absorption region caused by $Fe$ (1-2, 6 $\mu m$). In fact, taking into account the CLD contribution the experimental results obtained in works [21, 22] are described successfully by expression (10). The experimental results obtained in works [21, 22] and our calculated curves obtained by means of formula (10) are given in Fig. 7a, b, c.

## 5. Conclusions

Summing up the above mentioned we may draw the following conclusions:

1. It is necessary to take into account the possibility of the influences of growing optical birefringence and dichroism with investigations of quadratic and magnetooptic effects of the second order MLB and MLD in REIG crystals and epitaxial films, since their activities can essentially influence the anisotropy observed in the experiment and lead to incorrect conclusions.

2. The expressions for description of the principal indicatrix directions position for the magnetization rotation in the cubic crystal with the GOD and its principal axes random directions are obtained. It is shown, that obtained formulae describe well the experimental dependencies of principal dichroic directions in the REIG films. It gives evidence of correctness of quadratic magnetooptical effect phenomenologic description in the absorption region.

3. Investigations of the GOD spectra in YIG have shown that observed features in the spectrum are in the same wavelength range as in the absorption and the MLD spectra that is in the $Fe$ ion transitions. In *Bi*-substituted IG in the studied spectral region the GOD is displayed as the monotonous "tails" arising, apparently, from the high energy states.

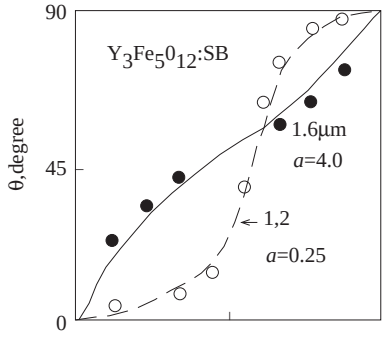


**(a)**

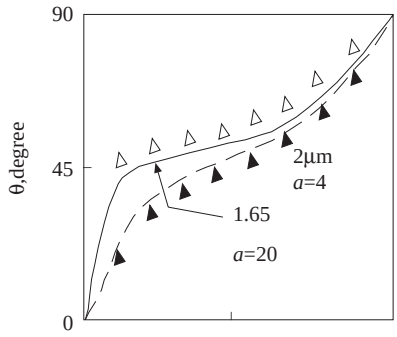


**(b)**

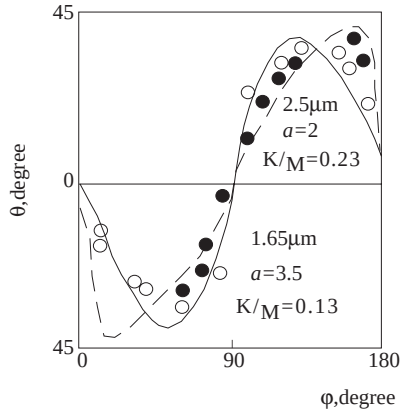


**(c)**

**Figure 7.** Dependences of dichroic axes rotation on magnetization position in (110) plane in the works [21, 22]. Solid and dashed curves are calculated

**Acknowledgement**

The author is grateful to Prof. Pisarev R.V. and senior scientific collaborator Krichevrov B.B. (Phisical & Technical Institute named after A.F. Ioffe, St. Petersburg) and Prof. Mukimov K.M. (Buchara State University, Buchara) for their interest in the work together with helpful discussions.

## References

[1] G.D. Smolensky, R.V. Pisarev, I.G. Siny, *Uspechi Fiz. Nauk*, **116** (1975) 231.

[2] J.F. Dillon, *Physics of Magnetic Garnets*, (Amsterdam 1978) p.379.

[3] A. Tucciatone, *Photoinduced Phenomena in Garnets in Physics of Magnetic Garnets*, ed. A. Paaletti (Amsterdam 1978) p.320.

[4] I.G. Siny, N.N. Kolpakova, Yu, M. Yakovlev, *Zh. eksper. teor. Fiz.*, **60** (1971) 2188.

[5] J. Ferre, G.A. Gehring, *Rep. Progr. Phys.* **47** (1984) 513.

[6] M.V. Berchenko, V.G. Veselaga, I. Cisilevski, S.N. Lyarhimets, A. Maziewski, S.G. Rudov, *Pisma v Zh. Ek. Teor. Fiz.*, **6**, (1993), 352.

[7] R.V. Pisarev, *Physics of Magnetic Dielectrics*, ed. G.A. Smolensky (Leningrad, 1974) p.153.

[8] G.S. Krinchik, V.D. Gorbunova, V.S. Guschin, *Zh. exper. teor. Fiz.*, **78**, (1980) 869.

[9] G.S. Krinchik, A.A. Kosturin, V.D. Gorbunova, *Zh. exper. teor. Fiz.*, **81**, (1981) 1037.

[10] J.F. Dillon, E.M. Gyorgy, J.P. Remeika, AIP Conference Proceeding 17th Annual Conference MMM (1971) p.190.

[11] R.V. Pisarev, N.N. Kolpakova, Yu M. Yakovlev, *Fiz. Tverd. Tela*, **14** (1972) 360.

[12] N.N. Kolpakova, R.V. Pisarev, M.J. Eganyan, *Fiz. Tverd. Tela*, **16** (1974) 1991.

[13] M.D. Sturge, J.P. Van-der Ziel, AIP Conf. Proc. 17th Ann. Conf. MMM (1972) p.195.

[14] G. Ya Guseinov, Sbornik trud. fiz. osnov microel. prib. (Moscow 1987) p.67.

[15] M. Manerie, A. Leclert, *Optics Com.* **16** (1976) 408.

[16] A.G. Ageev, E.V. Mokrushina, O.G. Rutkin, *Pisma v Zh. eksper. teor. Fiz.* **2** (1983) 328.

[17] B.B. Krichevzov, O. Ochilov, R.V. Pisarev, *Fiz. Tverd. Tela*, **25** (1983) 2404.

[18] F.V. Lisovsky, O.S. Markelova, V.I. Shapovalov, *Fiz. Tverd. Tela* **16** (1974) 3570.

[19] R.V. Pisarev, *Fiz. Tverd. Tela* **17** (1975) 1396.

[20] P. Feldman, T. Couzerh, H. Le Gall, *J. Appl. Phys.* **53** (1982) 8184.

[21] F. Lucazi, F. Terrenzio, G. Tomassetti, *J. Appl. Phys.*, **52** (1981) 2301.

[22] F. D'orazio, F. Luccazi, G. Tomassetti, *J. Magnet. and Magn. Mat.*, **31-34** (1983) 593.

[23] J.F. Hewkes, R.W. Teale, *J. Phys. C. Sol. St. Phys.* **5** (1972) 481.

[24] B. Antonini, S. Geller, A. Paoletti, *Phys. Rev. Lett.* **41** (1978) 1556.

[25] B.B. Krichevzov, O. Ochilov, R.V. Pisarev, *Pisma v Zh. eksper. teor. Fiz.*, **9** (1983) 950.

[26] R.D. Heury, E.C. Whitcomb, *Mat. Res. Bull.*, **10** (1975) 681.

[27] S.C. Parker, *Solid. Stat. Comm.* **31** (1979) 403.

[28] O. Ochilov, R.V. Pisarev, *Fiz. Tverd. Tela* **22** (1980) 2504.

[29] A.M. Balbashov, A. Ya Chervonenko, Magnetic Materials for Microelectronics (Moscow 1974) p.73.

[30] V.V. Rondoshkin, A. Ya Chervonenko, Applied magnetooptics (Moscow 1990) p.201.

[31] G.B. Scott, D.E. Lacklison, *J.L. Page, Phys. Rev.* **B12** (1975) 2562.

[32] D.E. Lacklison, G.B. Scott, B.H. Ralph, *Solid. St. Comm.* **10** (1972) 269.

[33] G.S. Krinchick, V.A. Krylova, E.V. Berdennikova, *Zh. eksper. teor. Fiz.* **65** (1973) 715.

[34] D.E. Larcklison, G.B. Scott, J.L. Page, *Sol. St. Comm.* **14** (1974) 861.

[35] G.B. Scott, D.E. Lacklison, *IEEE Trans. on magn.* **12** (1976) 192.

[36] O. Ochilov, Ph.D. Thesis, Institute of Nuclear Physics, Academy of Science, Tashkent, Uzbekistan 1984.

[37] O.B. Esikova, Ph.D. Thesis, Moscow State University, Moscow USSR, 1979.

[38] J.F. Dillon, J.P. Remeika, *J. Appl. Phys.* **41** (1970) 4613.

[39] B.B. Krichevzev, R.V. Pisarev, *Zh. eksper. teor. Fiz.* **84** (1983) 865.